

In vivo measurement of basilar membrane stiffness

Elizabeth S. Olson and David C. Mountain

Department of Biomedical Engineering, Boston University, Boston, Massachusetts 02215

(Received 4 June 1990; accepted for publication 26 November 1990)

Basilar membrane stiffness measurements were made in the base of the gerbil cochlea. Basilar membrane stiffness was determined by contacting the basilar membrane with a stainless steel needle (tip diameter 25 μm) attached to a force transducer, putting the needle/transducer structure through a low-frequency sinusoidal excursion with amplitude 5 or 25 nm, and measuring the restoring force exerted on the needle by the basilar membrane at the applied frequency. Stiffness was calculated as the amplitude of the restoring force divided by the amplitude of the excursion. Stiffness was measured over a 24- μm range of static displacements of the basilar membrane and is presented as stiffness versus static displacement. In cochleas that were not damaged during surgery the stiffness versus displacement characteristic usually had the following features: (1) an initial stiffness plateau with average stiffness 0.6 N/m; (2) a second plateau or level off with average stiffness 9.1 N/m; and (3) an increase in stiffness beyond the second plateau that was consistent with the theoretical stiffness-vs-displacement function of a beam. These features were present both pre- and post-mortem.

PACS numbers: 43.64.Kc, 43.64.Yp

INTRODUCTION

The basilar membrane is the underlying support of the organ of Corti. Its shape is that of a narrow, flat strip, tapering from the apex to the base of the cochlea. In ultrastructural observations in guinea pig, the basilar membrane was found to be composed of three anatomically distinct layers (Iurato, 1962). A layer of tympanic cells borders scala tympani. A 20-nm basement membrane forms the border with the organ of Corti. In between is a noncellular layer, composed of protein filaments in a cottony ground substance. The filaments run transversely between the osseous spiral lamina and the spiral ligament. The filamentous layer itself divides into two zones transversely. In the arcuate zone, between the lamina and the outer pillar cell, the filaments lie side by side beneath the basement membrane. In the transition region between the two zones, the filaments group into the bundles that characterize the pectinate zone, which is between the outer pillar cell and the ligament. The filament bundles complete the span to the ligament, which they enter. Light microscopic observations in the mongolian gerbil showed basic similarities to guinea pig with the exception that, in gerbil, the pectinate zone is unusually thick, seemingly due to an increased volume of cottony ground substance (Plassman *et al.*, 1987; Lay, 1972).

Voldrich (1978) demonstrated that when the basilar membrane was deflected with a needle, the form of the deflection was a thin radial depression. This observation, coupled with the transverse anatomy, suggested that the transverse filaments of the basilar membrane behave structurally as a set of transverse beams with little longitudinal coupling. Knowing the stiffness of the basilar membrane and the organ of Corti it supports is important to understanding the motion of the cochlear partition. The stiffness of these structures, coupled to the inertia of the fluid in the scalas, produces traveling wave motion in the cochlea. The ratio of partition stiffness to mass, a value that decreases from base to apex, determines how far along the basilar membrane the

traveling wave will go before it is rapidly attenuated.

Gummer *et al.* (1981) and Miller (1985) have measured basilar membrane point stiffness in freshly excised cochleas of guinea pig. However, it has recently been shown that the workings of the cochlea deteriorate almost immediately following death of an experimental animal (Rhode and Robles, 1974). This vulnerability was part of our motivation for making *in vivo* measurements, in which we could compare pre- to post-mortem stiffness. We also hoped to establish an experimental method that could become a basis for measuring forces in the cochlea.

The measurement was a dynamic measurement. A sinusoidal excursion was applied to a force transducer upon which a needle was mounted. The (flattened) tip of the needle was in contact with the basilar membrane. The force exerted on the needle by the basilar membrane was measured by the force transducer. The measurement was made over a range of static deflections. The stiffness at each static position was calculated as the amplitude of the force measured at that position, divided by the amplitude of the applied excursion. Because the measurement was dynamic, the quantity determined in this way is strictly the mechanical impedance of the basilar membrane, Z_m :

$$Z_m = F_a/x, \quad (1)$$

where F_a is the force applied by the needle to the basilar membrane in order to produce the motion x at the driving point. In complex terms,

$$Z_m = k - \omega^2 m + i\omega r, \quad (2)$$

where k is the stiffness, m is the mass, and r is the viscous resistance of the basilar membrane. We measure the force exerted on the probe by the basilar membrane, which is equal and opposite to F_a . The restoring force due to stiffness opposes the motion of the probe needle, i.e., is 180° out of phase with the motion. The force of inertia is in phase with the motion, while viscous resistance lags it by 90°. We measured

both the magnitude and phase of the force on the needle, and, in several experiments, measurements were made at more than one frequency. These measurements permit detection of viscous resistance and inertial forces. At the frequencies used, less than 100 Hz, the predicted inertial force due to a 25- μm section of the organ of Corti is several orders of magnitude lower than the force due to basilar membrane stiffness. Resistive forces in the basilar membrane are also expected to be relatively small. The mechanical impedance is expected to be dominated by stiffness, and our measurements bore this out. Therefore, we chose to use the term stiffness to describe the quantity we measure.

I. METHODS

Gerbils of the species *Meriones unguiculatus* (Mongolian gerbils) were used. The gerbil was given a subdermal injection of the analgesic tranquilizer acepromazine (dose 1 mg/kg) followed an hour later by an injection of the anesthetic sodium pentobarbital (initial dose 60 mg/kg). Supplemental 10-mg/kg doses of sodium pentobarbital were given when required. The temperature of the animal, measured with a rectal thermometer, was maintained at 38 °C. To maintain a clear airway, a slit was made in the trachea and a tracheal tube was inserted. The gerbil was on its back, with its head held in place with a headholder. Both pinnae were removed and cyanoacrylate glue between the gerbil's bullas and the earbars secured the animal's head into the holder. The left bulla was exposed by clearing away the overlying tissue with a hemostat and forceps and small scissors. The bulla was opened with sharp forceps and the bone of the bulla was removed as far medial and caudal as possible, and far enough rostral to allow for clear visibility of the round window opening of the cochlea. The cochlear bone surrounding the round window opening was scraped back approximately 100 μm with a small knife. The round window membrane was removed with a fine insect pin, bent at its tip to make a microhook. A tiny bit of dye (fast green FCF No. F-7252 Sigma) was put on the round window before its removal, to help visualize the membrane.

After a swath of the round window membrane had been removed, there was clear, approximately perpendicular access to the basilar membrane in the region where the membrane was entering the first turn. Figure 1 shows the approach to the basilar membrane. The measurement position was approximately 1.3 to 1.4 mm from the basal end of the basilar membrane. The entire length of the basilar membrane in this species of gerbil was measured by Plassman *et al.* (1987) as approximately 13 mm. The measurement position corresponded to approximately the 17-kHz best frequency place, based on measurements of summing potential made via an electrode in scala media (unpublished observation).

The rod extension of the force probe was securely clamped onto the endstage of a hydraulic microdrive, which was itself mounted onto a micromanipulator. The probe was manually positioned with the micromanipulator so that the end of the probe needle was inside the round window opening, and was pointed at, but roughly 70- μm up from, the basilar membrane. Further positioning of the probe was

done remotely from outside the sound chamber.

The force probe consisted of two parts: a force-to-voltage transducer which detected the forces on its attached needle and a voltage-to-motion transducer (driver) to produce the dynamic excursion and static displacement of the force transducer and attached needle. The needle was 1.8 cm long and tapered at the end to a flattened tip with a diameter of 25 μm . The probe stiffness was approximately 3500 N/m. This was much greater than the basilar membrane stiffness, so the needle's motion was not significantly diminished when loaded by the basilar membrane. The probe is described further in Appendix B.

The needle was aimed at the center of the basilar membrane widthwise (170 to 180 μm wide here), but, due to limited visibility, the true position of the needle was estimated as being centered to within half of the width. Given this estimation, our measurements were usually made in the pectinate zone of the basilar membrane, close to the transition between the arcuate and pectinate zones.

To make and determine contact the force transducer structure was put through a 35-nm peak sinusoidal excursion, and advanced toward the basilar membrane in 1- μm steps with the hydraulic microdrive until contact was detected: As soon as a stable peak emerged from the noise viewed on a spectrum analyzer, contact was assumed. The minimum detectable peak (with no averaging) corresponded to a force of roughly 10-nN peak, equivalent to a minimum detectable stiffness of 0.3 N/m.

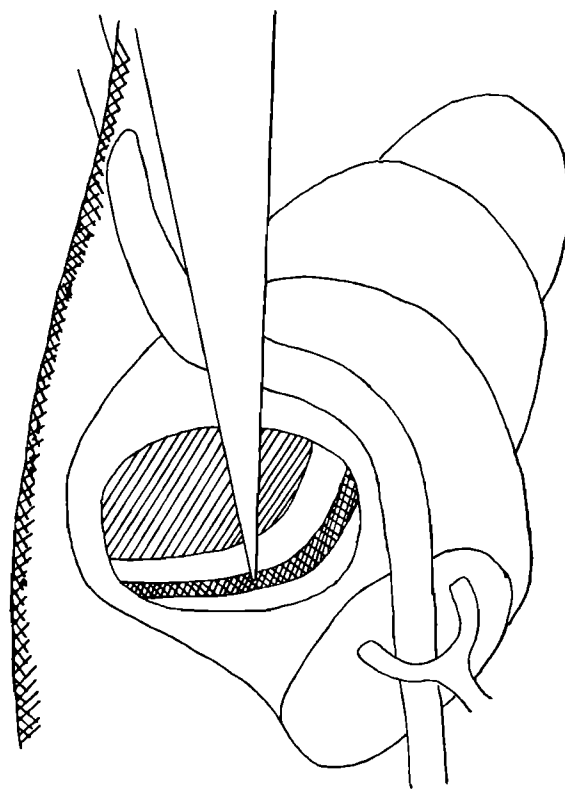


FIG. 1. Approach. View of cochlea after opening bulla. The probe needle is in contact with the basilar membrane, which appears as a dark stripe. The stapedial artery lies above the round window opening and continues through the opening in the stapes.

The force transducer structure was then stepped in $1\text{-}\mu\text{m}$ steps to a maximum static deflection of $20\text{ }\mu\text{m}$. It was then withdrawn in $1\text{-}\mu\text{m}$ steps to a $-4\text{-}\mu\text{m}$ position. A variation of this paradigm was sometimes performed in which the order of the static positions was pseudo-random. At each static position the probe was put through 30 presentations of a 5-nm peak sinusoidal excursion and 30 presentations of a 25-nm peak sinusoidal excursion. Each presentation was 0.9 s long. Most experimental runs were done at 80 Hz . Three runs were done with three consecutive frequencies of presentation at $20, 40, \text{ and } 80\text{ Hz}$.

During each excursion presentation, the transducer voltage was sampled 1500 times and the last 1024 samples were averaged over the 30 presentations. The averaged waveforms were stored in a PDP-11 computer and were Fourier analyzed for the magnitude and phase of the return force.

Mechanical noise, the dominant noise source, was attenuated by doing the experiments on a vibration isolation table in a sound chamber. The general noise level in the $20\text{- to } 200\text{-Hz}$ range of frequencies that was monitored during experiments with a spectrum analyzer was at level corresponding to a force of approximately $3.6\text{ nN}(\text{rms})/\sqrt{\text{Hz}}$. The background noise level in the spectra of computer analyzed data was at a level of $0.6\text{ nN}(\text{rms})/\sqrt{\text{Hz}}$.

As a monitor of cochlear health, the compound action potential (CAP) response to tone bursts spanning the frequencies from $2\text{-}20\text{ kHz}$ at levels of $50, 60, \text{ and } 70\text{ dB SPL}$ was measured. The CAP was measured via a silver wire electrode positioned just outside the round window opening. The response was measured before the bone of the round window opening was cleared and the round window membrane removed, again just after round window removal, and at interim periods during the experiment.

A. Sources of experimental error

It is possible for a drop of water to condense onto the upper portion of the needle midway through a stiffness measurement, which would exert an inertial force on the needle. For example, at 80 Hz the mass required to produce an inertial force with magnitude equivalent to a stiffness of 1 N/m is 4 mg , corresponding to a volume of water of 4 mm^3 . Drops this large were never seen. An inertial force produced in this way would be detected as an error when the forces on the needle were checked following the stiffness run. Runs in which the post-run error was found to be substantial were excluded from the reported results.

The dynamic force on the needle due to surface tension at the fluid/air interface is predicted to be in phase with excursion, with a magnitude of approximately 0.1 N/m multiplied by the excursion size. With the excursion sizes used a force of this size is at or beneath the level of the noise. Trials designed to detect the force of surface tension, in which the needle was lowered into water or watery gelatin, did not produce a detectable signal.

A deviation from perpendicular contact between the probe and the basilar membrane would introduce two errors. First, the measured stiffness would be equal to the actual stiffness multiplied by a factor $\cos(\theta)$, where θ is the deviation angle. Theta was estimated as being less than or equal

to 15° , producing a maximum error in the measured stiffness of 5% . Second, a deviation from perpendicular contact would cause the edge of the probe to make initial contact with the basilar membrane, so not all the fibers in the $25\text{-}\mu\text{m}$ basilar membrane section eventually contacted by the probe would be engaged at once. As the probe was advanced more fibers would become engaged. This would result in a region of increasing stiffness. A 15° error would produce a region of increasing stiffness lasting $3\text{ }\mu\text{m}$. Therefore, a deviation from perpendicular contact might be partly responsible for the region of increasing stiffness we attribute to probe coupling in the presentation of results below.

II. RESULTS

Basilar membrane stiffness measurements were performed in 18 gerbils. We emphasize the results from the most recent 12 gerbils, in which measurements were made with the paradigm described above. Before presenting the results of the basilar membrane stiffness measurements, we present observations on the extent of the damage caused by the experiments.

Two of the 12 cochleas were damaged during removal of the round window membrane. Damage was immediately known, and as expected, caused severe reduction in the CAP response. In cochleas in which round window removal appeared to be successful, the CAP response usually was not substantially reduced following removal. In all but one experiment the CAP was severely reduced following the first stiffness measurement. In Fig. 2(a) ratios of the CAP responses to 60-dB SPL tones after round window removal to the responses before round window removal are shown. The ratios are plotted for a gerbil in which round window removal was successful (731) and for a gerbil in which damage occurred (102). In animal 102, the ratios are small across frequencies, while, in animal 731, the ratios are always greater than 0.7 . In Fig. 2(b) the ratios of the CAP responses to 60-dB SPL tones after the first stiffness run to the responses before the first stiffness run, but after round window removal are shown for two gerbils which had successful round window removal. The ratios for animal 731 show what typically occurred following the first stiffness run: The CAP ratios are small across frequencies. In contrast, the CAP responses of animal 016 were still relatively strong following the run. In animal 016, the CAP was still viable after the second run, but following the third run the CAP response was severely reduced. In one experiment an electrode was inserted into scala media, allowing for monitoring of the endocochlear potential. The endocochlear potential was stable at 58 mV for over half of the first stiffness run but then fell gradually, and was 46 mV at the end of the run. Following the run, the CAP response was substantially reduced, especially at high frequencies.

In the 12 experiments, round window removal was successful in animals 717, 731, 87, 109, 016, 031, N27, D4, and D11. Damage occurred during round window removal in cochleas 87 and 102. In animal 722, although round window removal was successful, localized damage to the basilar membrane occurred during positioning of the probe. (Re-

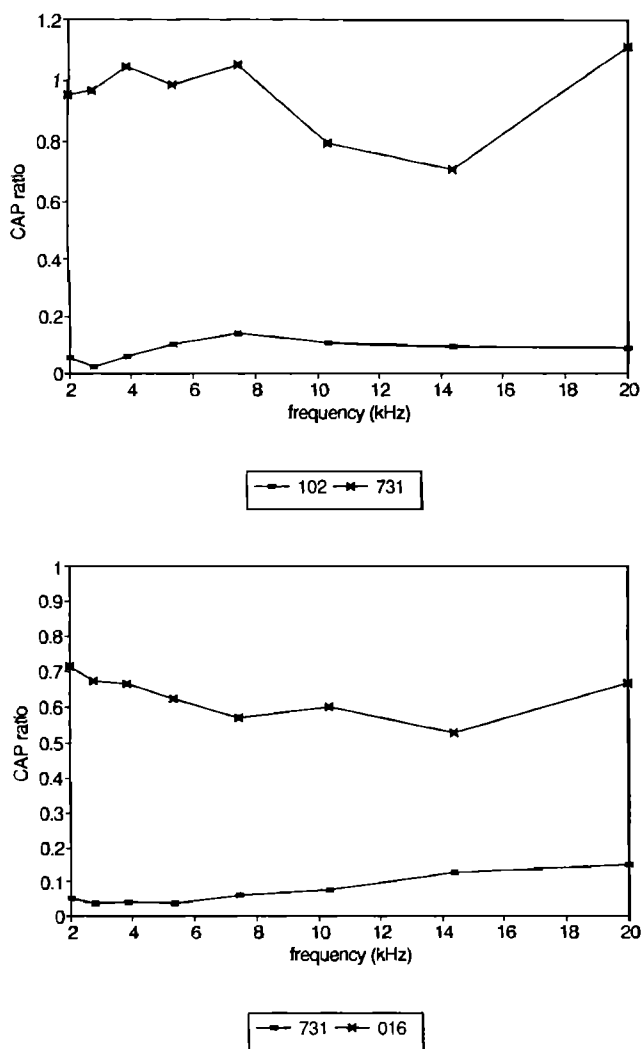


FIG. 2. (a) Ratios of CAP responses to 60-dB SPL tones after to responses before round window removal in two animals. (b) Ratios of CAP responses to 60-dB SPL tones after to responses before first basilar membrane stiffness run in two animals.

sults from all 12 cochleas are included in the pooled data in Fig. 7.)

Most experiments contained four to five stiffness runs. In all but a few cases, the probe was repositioned between runs. The last one to two runs of an experiment were sometimes done after the animal was sacrificed with an overdose of sodium pentobarbital. Measurements in which the null of the transducer inertia was not stable over the course of the run (see Appendix B); measurements in which no change in force was measured throughout the run, likely due to erroneous judgment of contact; and measurements in which the probe was accidentally positioned very close to the lamina or ligament, are not included in the pooled data. From the 12 animals, we include data from 39 stiffness runs.

In general, the force exerted on the probe by the basilar membrane was very close to 180° out of phase with the excursion. The absence of a lagging force component indicates the absence of a significant contribution to the force from viscous resistance. In experiments in which force was measured at 20, 40, and 80 Hz, the stiffnesses measured at the three

frequencies were approximately equal, indicating that inertial forces were insignificant at these frequencies. Therefore, the data are presented as stiffness (k) versus static displacement (x) curves, where k is calculated as the force amplitude divided by the excursion amplitude. The phase of the force relative to the excursion is plotted along with each magnitude plot.

A. Typical features of basilar membrane stiffness

In cochleas that were not damaged during round window removal the stiffness versus displacement characteristic displayed typical features. The common features of basilar membrane stiffness are numbered in Fig. 3(a) (animal 016 run 1) with the numbers corresponding to the regions described below.

1. Initial plateau

Twenty-one out of 39 runs had an initial plateau. The plateau varied in length between 2 and $12 \mu\text{m}$, with a mean

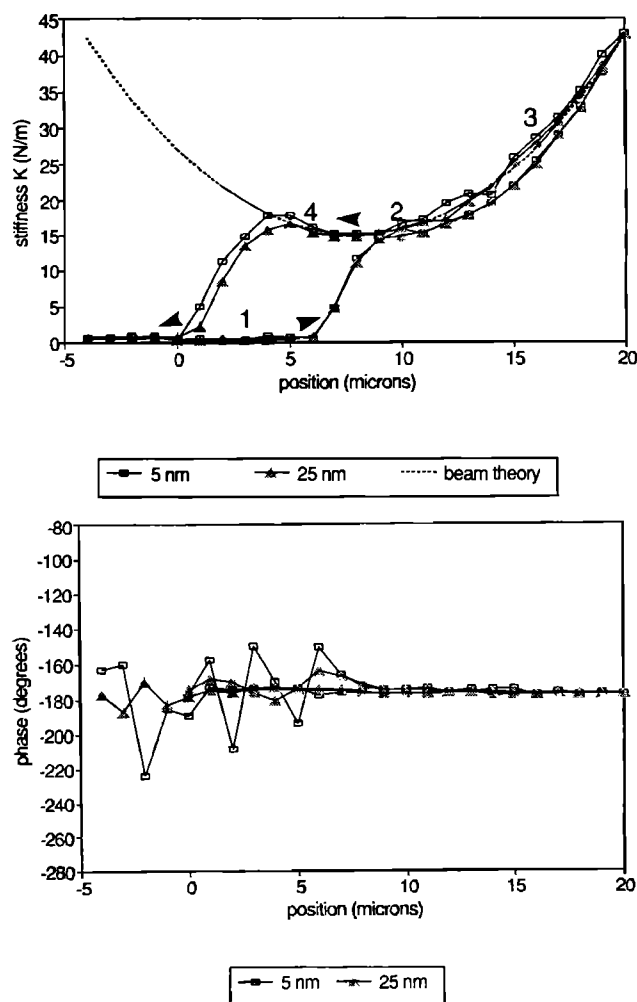


FIG. 3. Basilar membrane stiffness (top) and phase of force relative to excursion (bottom). Data from one stiffness run is plotted. Arrows differentiate data taken as probe was advancing from data taken as probe was retracting. Features that were common to most measurements are identified with numbers. (1) Initial plateau; (2) second plateau; (3) final quadratic growth in stiffness, and (4) extension of second plateau as probe is retracted. The quadratic fit to the data is $k = 15 \text{ N/m} + 0.19 \text{ N}/(\text{m} \mu\text{m}^2)(x - 8.0)^2$.

length of $4.6\ \mu\text{m}$, and had a stiffness that ranged between 0.2 and $1.2\ \text{N/m}$, with a mean stiffness of $0.6\ \text{N/m}$. The length of the initial plateau was influenced by background noise, which was often dominated by animal noise and varied between experiments. There is a correlation between noise and plateau length because, in noisy experiments, the basilar membrane was probably not detected until it had been deflected a relatively large distance. The initial plateau was relatively short and sometimes absent in noisy experiments.

2. Second plateau

Thirty-three out of 39 runs had a second plateau. In measurements in which the static position of the probe was advanced in order, a rise in stiffness lasting from 2 to $6\ \mu\text{m}$ usually occurred beyond the initial plateau, ending in a region where the stiffness was almost constant with displacement. The stiffness of this second plateau region ranged from $1.4\text{--}20\ \text{N/m}$, and was on average $9.1\ \text{N/m}$. Four of the largest second plateau stiffnesses, with values of 15, 16, 17, and

20, were found in animal 016. One explanation for the rise to the second plateau is that the probe was becoming fully coupled to the basilar membrane over the rise region. To test this explanation, a variation of the standard run was done in which the order of the static positions was randomized. Results from two consecutive measurements made at the same location are shown in Fig. 4 (animal D11, runs 1 and 2). The first run, Fig. 4(a), was done with randomly ordered static positions. In this case, following the $0\text{-}\mu\text{m}$ position, the needle was advanced to the $8\text{-}\mu\text{m}$ position. The second run, Fig. 4(b), was done with ordered static positions. The two stiffness measurements gave similar results. However, the gradual rise in stiffness that occurred between the contact point and the $6\text{-}\mu\text{m}$ position in Fig. 4(b) is absent in Fig. 4(a). These data support the explanation that the rise to the second plateau found in the ordered measurements was due to probe coupling and that the rise was absent in random measurements because the initial $8\text{-}\mu\text{m}$ displacement fully coupled the probe to the basilar membrane.

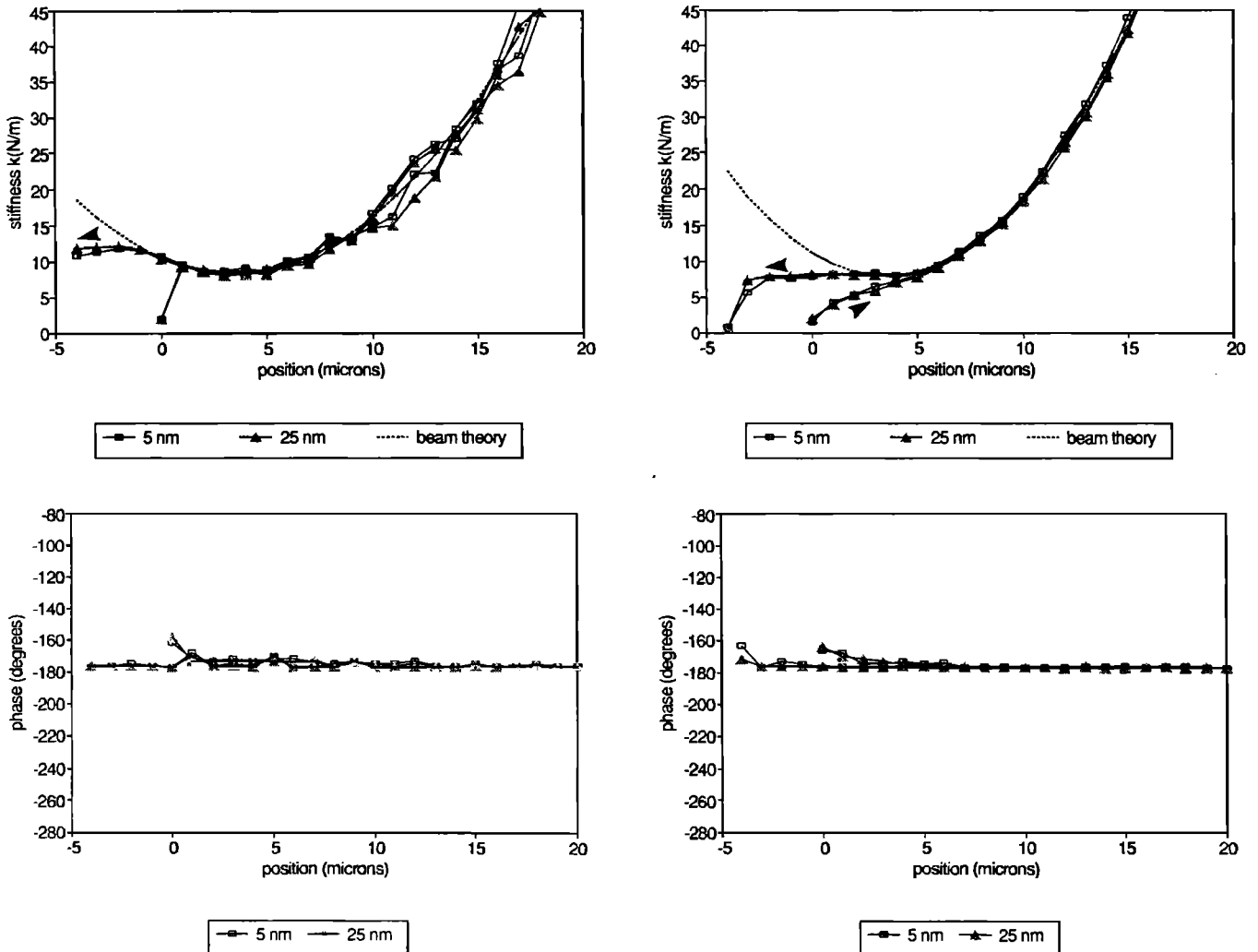


FIG. 4. (a) Basilar membrane stiffness (top) and phase of force relative to excursion (bottom). Measurement made with randomized static positions. The static positions were ordered as follows: 0, 8, 19, 4, 17, 2, 11, 13, 10, 6, 12, 20, 3, 7, 16, 14, 1, 18, 9, 15, 5, then reversed (5, 15...), and finally, $-1, -2, -3, -4$. Quadratic fit to the data is $k = 8.5\ \text{N/m} + 0.18\ \text{N}/(\text{m}\ \mu\text{m}^2)(x - 3.5)^2$. (b) Basilar membrane stiffness (top) and phase of force relative to excursion (bottom). Measurement made with ordered static positions, immediately after, and in same position as, measurement of (a). Quadratic fit to the data is $k = 8.0\ \text{N/m} + 0.26\ \text{N}/(\text{m}\ \mu\text{m}^2)(x - 3.5)^2$.

3. Final growth

Following the second plateau the stiffness increased smoothly, with a form that can be fitted with the quadratic function

$$k = k_p + a(x - x_p)^2. \quad (3)$$

This is the theoretical stiffness versus displacement relationship of a beam, where k_p is the beam's linear stiffness, x_p is the undeflected position of the beam and a , the coefficient of the quadratic term, is dependent on the dimensions, boundary conditions, and material of the beam (Gummer *et al.*, 1981). In Figs. 3, 4, and 6 fits of the quadratic function to the data are shown.

4. Extension of the second plateau as the probe was retracted

In many cases, as the probe was retracted, the second plateau was extended to static displacements smaller than the static position of its onset as the probe was advanced. This was probably because the probe was fully coupled to the basilar membrane over the full second plateau region as the probe was retracted. In 17 runs, the plateau was extended to the point that the stiffness increased, as though the basilar membrane were stuck to and being retracted with the needle.

In some cases as the probe was retracting, at static displacements just smaller than the region of the second plateau extension there was a region in which the stiffness scaled nonlinearly with excursion level. The range from 0–6 μm , retracting, in Fig. 3 provides a clear example. The smaller (5 nm) excursion gave a larger stiffness than the larger (25 nm) excursion. In this case, the 5-nm excursion was made before the 25-nm excursion. In runs in which the 25-nm excursion was made first, it gave a larger stiffness in this region of the curve. The steep portion of the curve retracting seems to represent the uncoupling of the probe from the basilar membrane, and apparently whichever excursion level occurs later measures a reduced stiffness because of a slightly less coupled probe. The nonlinear points did not have significant harmonics as they would if they represented positions at which the probe was completely uncoupled from the membrane, and was actually knocking up against it.

The phase of the force on the needle relative to the excursion phase in Fig. 3 was close to 180° throughout the run. The first few and last few measurements made with the 5-nm excursion show the largest deviations from 180° . The forces in these measurements were almost in the noise.

Cochleas 816, 102, and 722 did not possess the basilar membrane stiffness versus displacement characteristic that was found in cochleas that were not damaged during round window removal. In cochleas 816 and 102, the second plateau was absent or less pronounced and the stiffness was in general smaller. Figure 5 shows a stiffness versus displacement plot from experiment 102 (run 5).

In cochleas that were healthy following round window removal, the features of early post-mortem stiffness (less than 2 h post-mortem) were similar to the features of pre-mortem stiffness described above. Figure 6 shows two stiffness versus displacement measurements from animal 731 (runs 4 and 5). Figure 6(a) was a pre-mortem measurement

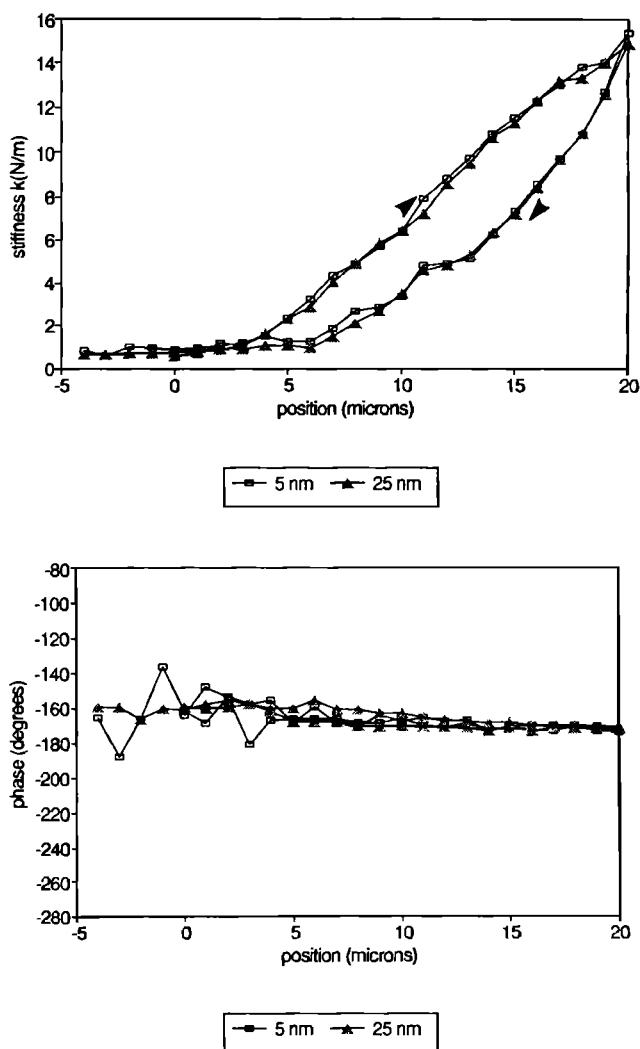


FIG. 5. Basilar membrane stiffness (top) and phase of force relative to excursion (bottom) in a damaged cochlea.

and Fig. 6(b) was an early post-mortem measurement. The rise to the second plateau and final quadratic increase in stiffness as the probe was advanced, and extension of the second plateau as the probe was retracted are apparent in both plots. The differences in the two plots do not exceed differences between pre-mortem runs. In Fig. 6(a), the stiffness when the probe was retracted was smaller than when the probe was advanced. Hysteresis of this sort occurred commonly both pre- and post-mortem.

Characteristics of the stiffness versus displacement measurements from the 12 animals are pooled in Fig. 7. We graph histograms of incidence of measurements of stiffness within given ranges for the stiffness at the 20- μm position, and for the stiffnesses of the first and second plateaus. A spread in the measured basilar membrane stiffnesses is to be expected for the following reasons: We have estimated that the needle tip is positioned within 50% of the center of the basilar membrane widthwise. This variability in transverse centering of the probe is expected to cause variability in the measured stiffness of both plateaus and the stiffness at the 20- μm position. Miller (1985) made stiffness measurements across the width of the basilar membrane, and found that the

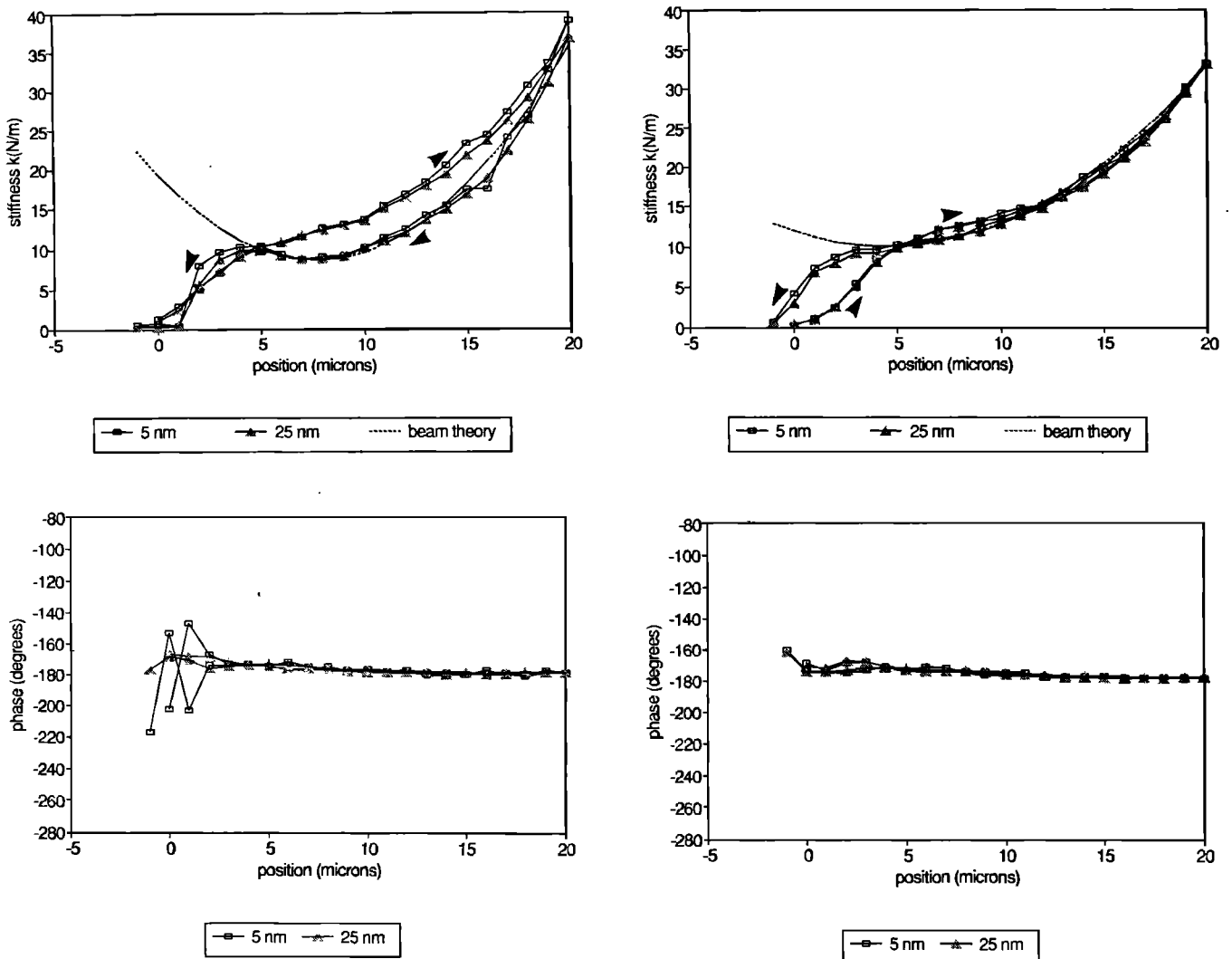


FIG. 6. (a) Basilar membrane stiffness (top) and phase of force relative to excursion (bottom). Pre-mortem stiffness measurement. Quadratic fit to the data is $k = 8.6 \text{ N/m} + 0.18 \text{ N/(m } \mu\text{m}^2)(x - 7.75)^2$. (b) Basilar membrane stiffness (top) and phase of force relative to excursion (bottom). Post-mortem stiffness measurement made after measurement of (a). Quadratic fit to the data is $k = 10.0 \text{ N/m} + 0.095 \text{ N/(m } \mu\text{m}^2)(x - 4.5)^2$.

stiffnesses were greater by factors of 1.3 to 3 in the positions one-quarter and three-quarters across the width of the membrane relative to the stiffness midwidth. A second source of variation is that, as stated in the initial plateau description above, the stiffness, and thus the deflection, with which a run begins is partly dependent upon the noise level. Variability in the deflection with which the run begins will cause variability in the value of the stiffness at the 20- μm position.

B. Stiffness of the spiral lamina

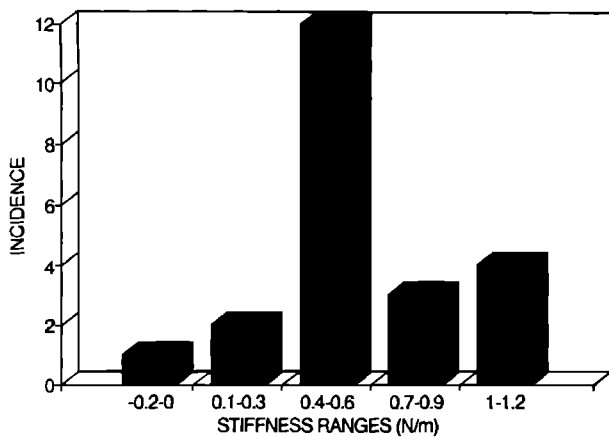
In experiments O31 and N27, the stiffness of the bone of the spiral lamina was measured by positioning the needle tip over the lamina, close to its connection with the basilar membrane. In both measurements, following an initial 1- to 2- μm region of increasing stiffness, probably due to coupling of the probe to the lamina, the lamina stiffnesses were roughly constant over at least 9 μm of static deflection. The lamina

stiffnesses were 10 070 N/m and 16 800 N/m. These stiffnesses were determined by taking into account the degree to which the lamina stiffness loads the probe, whose stiffness is 3500 N/m. The large value of lamina stiffness relative to basilar membrane stiffness suggests that the bone provides a rigid edge support for the basilar membrane.

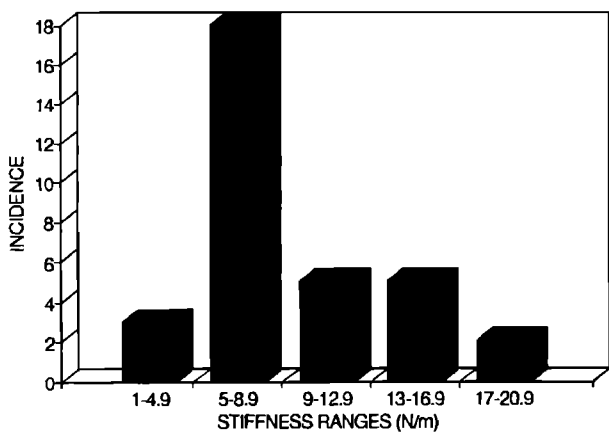
III. DISCUSSION

A. Comparison with point stiffness measurements made in excised cochlea of guinea pig

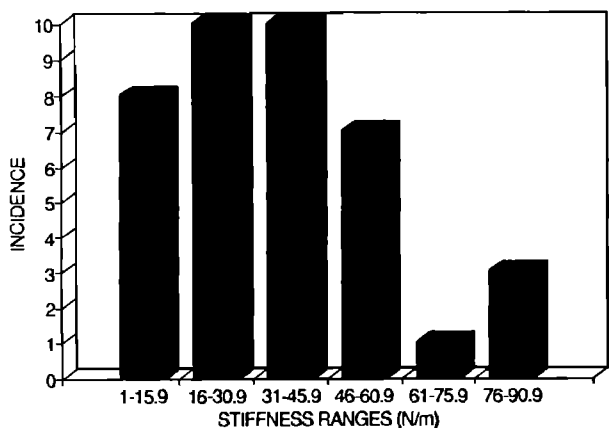
One of the reasons for doing *in vivo* experiments was to look for differences in stiffness pre- and post-mortem. Our own observations of pre- versus post-mortem stiffness showed that the typical features of stiffness did not depend on the animal being alive. Therefore, we might expect the stiffness we measure to be similar to the stiffness measured in excised cochleas. A relevant anatomical difference should be



(a)



(b)



(c)

FIG. 7. Stiffnesses of different regions, pooled across data; (a) Initial plateau stiffness; (b) second plateau stiffness; and (c) stiffness at 20- μm position.

noted. The anatomy of the basilar membrane of most gerbil species, including *Meriones unguiculatus*, has a specialized structure that is not found in guinea pigs or most other mammals. This is a relatively thick basilar membrane, especially in the pectinate zone, due to what was described by Lay

(1972) as a “hyaline mass.” This tissue forms a layer of the basilar membrane with the transverse filaments, with which it is enclosed and sparsely threaded. Lay suggested that the hyaline mass might be an increased volume of the cottony ground substance described in Iurato’s (1962) ultrastructural studies. A thick basilar membrane is expected to be stiffer than a relatively thin basilar membrane. On the other hand, the hyaline mass might not contribute to the basilar membrane stiffness as much as other components, in particular, the transverse protein filaments and possibly the organ of Corti. Plassman *et al.* (1987) argue against the hyaline mass contributing to basilar membrane stiffness, using as evidence that the greatest thickening occurs in the medium- and low-frequency regions of the cochlea, and that the gerbil species with the greatest sensitivity to low frequencies possess the largest hyaline mass beneath the pectinate zone.

Both Gummer *et al.* and Miller reported a stiffness plateau upon contacting the basilar membrane that usually persisted over the first 2 to 3 μm of static basilar membrane displacement. Gummer *et al.*’s values of early plateau stiffness varied between 0.25 and 0.8 N/m. Miller’s values of early plateau stiffness varied between 0.4 and 2.0 N/m. (Miller made measurement with a 10- μm -diam probe needle. In a beam model of the basilar membrane, stiffness scales with probe diameter so to compare her results with ours we multiplied the stiffnesses she reported by 2.5. Miller made measurements across the width of the basilar membrane. We only included her measurements that were centered to within half of the basilar membrane width in this comparison.) Our initial plateau stiffness ranged between 0.2 and 1.2 N/m and persisted over as many as 12 μm , with a mean length of 4.6 μm . The size of the initial plateau stiffness is fairly similar in Miller’s, Gummer *et al.*’s, and our measurements, and its length is greatest in our measurements.

Miller reported that the stiffness versus displacement relationship (which she measured over 10 μm) had three plateaus. The third, stiffest plateau had a stiffness of approximately 1.4 to 12.5 N/m. Our second plateau stiffness, which ranged from 1.4–20 N/m, with a mean of 9.1 N/m, is similar to Miller’s third plateau. Gummer *et al.* did not report a plateau above the initial plateau, but did observe a “saturation” in stiffness increase. However, the saturation occurred at a stiffness of approximately 2 N/m, significantly lower than the plateaus Miller and we measured. The stiffnesses reported by Gummer *et al.* were similar to stiffnesses we have measured in cochleas which were damaged during round window removal, and it is possible that their measurements were made on cochleas that had been similarly damaged.

B. Interpretation of different regions of measured stiffness

A schematic of a cross section of the organ of Corti shown in Fig. 8 illustrates a tentative interpretation of the different stiffness regions. The initial plateau [Fig. 8(b)] is interpreted as the stiffness of structures which have low resistance to shear but are possibly incompressible, and is ten-

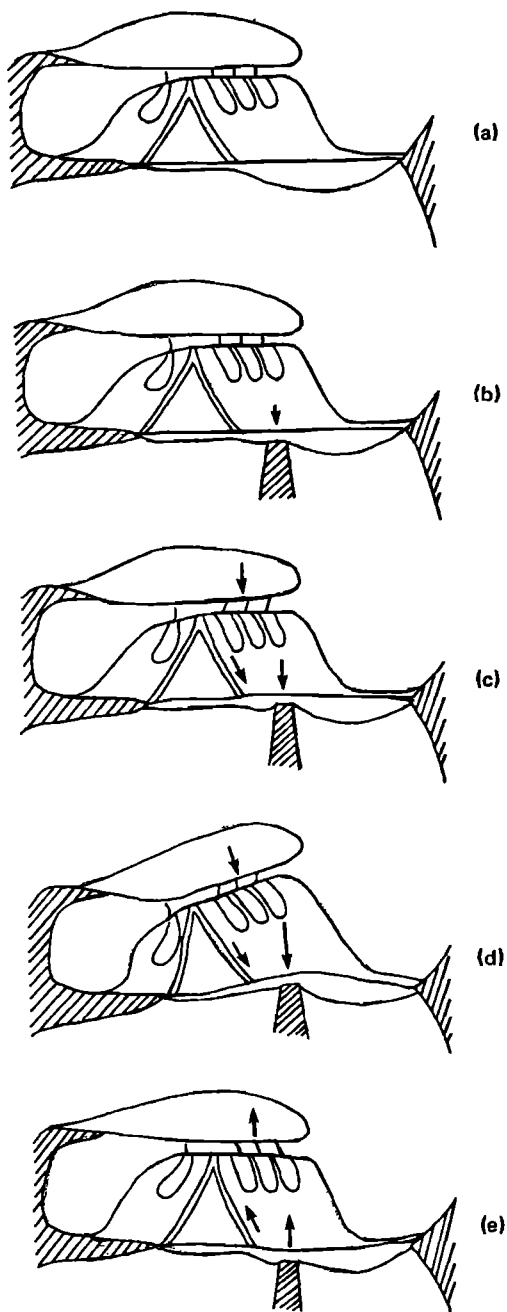


FIG. 8. Speculative anatomical basis for different regions of basilar membrane stiffness. Arrows designate restoring forces. (a) Cross section of the organ of Corti prior to probe contact; (b) initial plateau region of stiffness; (c) second plateau region; (d) final quadratic growth in stiffness; and (e) extension of second plateau as probe is retracted.

tatively identified with the hyaline mass, or cottony ground substance described above. This interpretation of the initial plateau was put forth by Miller (1985). The greater length of the early plateau in our measurements relative to measurements in guinea pig might reflect the greater thickness of this layer in gerbil.

As Miller pointed out, if the initial stiffness plateau is due to an incompressible substance, under pressure loading, the substance's stiffness would be very large compared to the stiffness due to the deformation of cochlear structures and it

would not contribute to the stiffness relevant to cochlear mechanics. Then the structures that give rise to the second stiffness plateau might provide the relevant stiffness. The structures that give rise to the second plateau [Figs. 8(c) and (e)] are not known. It is possible that the second plateau is the linear stiffness region of the transverse protein fibers of the basilar membrane, but we cannot rule out a contribution to the stiffness from the organ of Corti. In Miller's measurements, in which hair and supporting cells were not intact, the arches of Corti apparently contributed to the measured stiffness. In our experiment 016, the CAP response to high-frequency tones was still viable following two stiffness runs, suggesting that hair cells and their attachments were probably intact in at least this animal, which had the largest average second plateau stiffness. Therefore, in panels (c) and (e), we include a contribution to the second plateau stiffness from structures of the organ of Corti, with possible contributions from hair cells and their attachments. The values of stereocilia stiffness determined by Strelioff and Flock (1984) and Howard and Huspeth (1988), when adjusted to the geometry and dimension of the outer hair cell stereociliary bundle, indicate that the stereociliary contribution to the stiffness we measure could be of the order of a N/m, thus making a significant contribution to the second plateau stiffness.

Beyond the second plateau, the stiffness increases quadratically with distance [Fig. 8(d)]. A quadratic stiffness-deflection relationship is the signature of a structure with attached edges that is deflected to the extent that there is a nonlinear dependence of restoring force on deflection due to stretching. The transverse protein filaments have a beamlike structure and firm edge attachments, and are the most probably basilar membrane component to produce the quadratic increase in stiffness.

We have suggested that the second plateau stiffness is produced by structures of the organ of Corti in addition to the transverse filaments of the basilar membrane, while the quadratic growth in stiffness following the plateau is produced predominantly by the filaments. Analysis of the data supports this proposal. The k_p and a values found in fitting the beam equation (3) to the data can be used to calculate the beam height. The size of the calculated beam height can be used to bound the possibilities for the sources of the second plateau and quadratic growth in stiffness. (Allaire *et al.*, 1974; Bummer *et al.*, 1981.) In particular, if the quadratic growth in stiffness is due to the protein filaments, but the plateau stiffness is due to other structures in addition to the filaments, the calculated beam height will be larger than the anatomical height of the filaments.

The calculation of beam height depends on the location and area of force application and on the boundary conditions of the beam. Gummer *et al.* derived the expression for beam height for a beam with a force applied at its midpoint with either simply supported or clamped boundary conditions. They favored the clamped condition, whereas other authors (Miller, 1985; von Békésy, 1960) have favored boundary conditions in which the lamina edge is clamped and the ligament edge is simply supported. The calculated beam height with one edge clamped and one edge simply supported is intermediate between the calculated height with simply sup-

ported edges and the calculated height with clamped edges. Using Gummer *et al.*'s derived equation with our probe tip diameter ($25\ \mu\text{m}$) and our measured basilar membrane width ($175\ \mu\text{m}$) gives for the apparent beam height: (1) clamped condition $h = 1.4 (k_p/a)^{0.5}$, and (2) simply supported condition $h = 5.0 (k_p/a)^{0.5}$.

These expressions and the k_p and a values found from fits to the stiffness versus displacement measurements in Figs. 3, 4, and 6 were used to calculate the beam heights in Table I. With the clamped condition, the heights range from $7.8\text{--}14.4\ \mu\text{m}$; with the simply supported condition, the heights range from $27.8\text{--}51.4\ \mu\text{m}$. The thickness of the pectinate zone of the basilar membrane in *Meriones unguiculatus* is roughly $10\ \mu\text{m}$ in the extreme base of the cochlea but increases in turn 1 to approximately $20\ \mu\text{m}$ (Plassman *et al.*, 1987; Lay, 1972). Our measurements were made in the transition between these two regions. However, based on the anatomical observations in guinea pig by Iurato, and those in gerbil by Plassman *et al.* and Lay, the transverse protein filaments probably account for only a few μm worth of the thickness. Therefore, the calculated beam heights are large compared to the anatomical thickness of the transverse protein filaments of the basilar membrane, suggesting that structures other than the transverse filaments contribute to k_p .

Several of our basilar membrane stiffness measurements had particular features that supported the proposal that the structures that produce the stiffness of the second plateau are different from the structures that produce the stiffness beyond the plateau. For example, Fig. 9 (animal N27, run 1) shows a basilar membrane stiffness measurement in which the probe was positioned close to the lamina. As the probe was advanced, the stiffness increased quickly, but smoothly. As the probe was retracted the stiffness decreased more quickly than it had increased, as though the basilar membrane had been stretched out by the measurement. Possibly because of this reduced stiffness, a plateau that was not apparent as the probe was advanced was apparent as the probe was retracted. The plateau had a stiffness of $16.5\ \text{N/m}$, which is within the bounds of the plateau stiffnesses found in measurements made midwidth on the basilar membrane. That the plateau stiffness was affected less by the off-centered position of the needle than the region of increasing stiffness beyond the plateau suggests that different structures contributed to the two stiffness regions.

TABLE I. Apparent height of basilar membrane beam structure, calculated from fits of beam Eq. (3) to the data.

Measurement	k_p (N/m)	a (N/m μm^2)	Calculated height (μm)	
			Clamped	Simply supported
Fig. 3	15.0	0.19	12.4	44.4
Fig. 4(a)	8.5	0.18	9.6	34.3
Fig. 4(b)	8.0	0.26	7.8	27.8
Fig. 6(a)	8.6	0.18	9.7	34.6
Fig. 6(b)	10.0	0.095	14.4	51.4

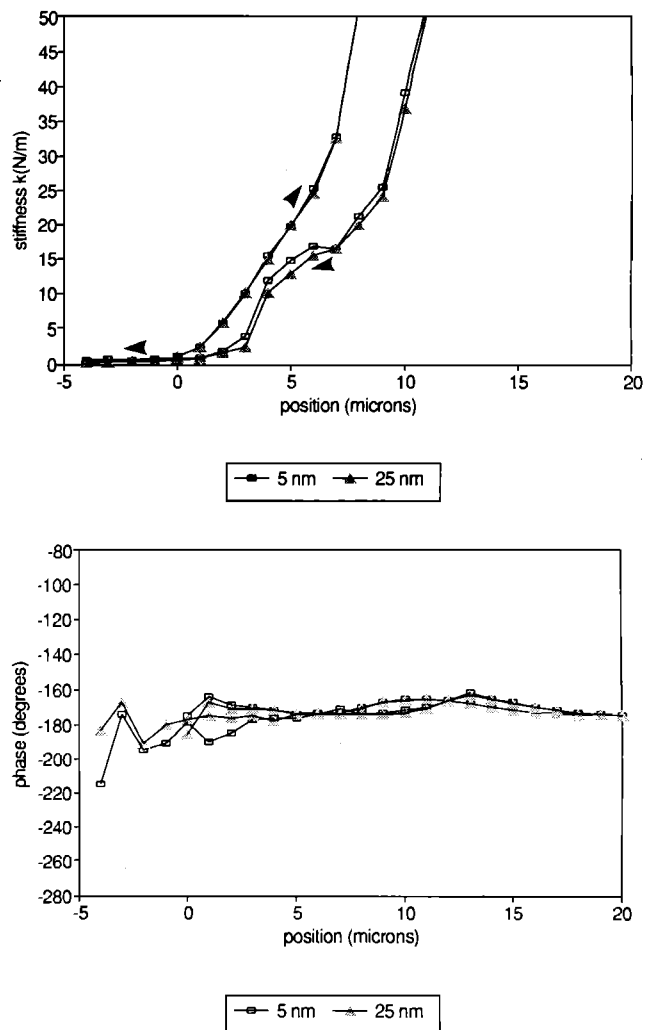


FIG. 9. Basilar membrane stiffness (top) and phase of force relative to excursion (bottom).

C. Calculation of volume compliance

Our measurements of point stiffness can be used to estimate the volume compliance of the basilar membrane. Volume compliance is equal to the displaced volume of fluid per unit basilar membrane length divided by the pressure across the basilar membrane. Because pressure across the basilar membrane is the physiological input driving basilar membrane motion, knowing the volume compliance is important for models of cochlear mechanics.

$$\text{volume compliance} = A/P, \quad (4)$$

where A is the cross sectional area of the displaced fluid, and P is the pressure across the membrane;

$$\text{point compliant} = x/F, \quad (5)$$

where x is the displacement of the beam at a point and F is the force applied at that point. Point compliance is the inverse of point stiffness. We found the point stiffness of the second plateau, which we interpret as the relevant stiffness for cochlear mechanics, to be approximately $9.1\ \text{N/m}$. Expressed as point compliance, it is $0.11\ \text{m/N}$.

In order to use point compliance to calculate volume compliance, we approximate the length of basilar membrane

that is deflected by the probe as a beam, and use linear beam theory. The width of the beam is equal to the width of the probe: Because of the assumption of little longitudinal coupling in the basilar membrane, the adjacent regions are assumed to not be deflected. The length of the beam is equal to the transverse width of the basilar membrane, bounded by the spiral ligament on one side and the spiral lamina on the other. We have found volume compliance as a function of point compliance for both simply supported and clamped boundary condition. An outline of the calculations is given in Appendix A. Here, we give the results:

(1) clamped boundary condition:

$$\text{volume compliance} = \text{point compliance} \times (2.2 \times 10^{-13} \text{ m}^3);$$

(2) simply supported boundary condition:

$$\text{volume compliance} = \text{point compliance} \times (3.1 \times 10^{-13} \text{ m}^3).$$

Using our 0.11-m/N value of point compliance we find:

(1) clamped boundary condition:

$$\text{volume compliance} = 2.4 \times 10^{-14} \text{ m}^4/\text{N}$$

(2) simply supported boundary condition:

$$\text{volume compliance} = 3.4 \times 10^{-14} \text{ m}^4/\text{N}.$$

These values of volume compliance can be compared to volume compliances in a table compiled in Ruggero *et al.* (1990). They calculated volume compliance by combining results from basilar membrane motion measurements with results from intracochlear pressure measurements. For example, in guinea pig, the volume compliance they calculated by combining Sellick *et al.*'s (1982) motion measurements (made 0.34 cm from the stapes) and Dancer and Frank's (1980) pressure measurements was $6.4 \times 10^{-14} \text{ m}^4/\text{N}$. In cat, motion measurements 0.3 cm from the stapes (Khanna and Leonard, 1986) and Nedzelnitsky's (1980) pressure measurements were used to calculate a volume compliance of $1.8 \times 10^{-14} \text{ m}^4/\text{N}$. Our calculated volume compliance is similar to these volume compliances. The variability in the volume compliances might be due to species differences and differences in the characteristic frequencies (cf) of the measurement positions; Khanna and Leonard's motion measurements in cat were made at positions with cf generally greater than 20 kHz, whereas Sellick *et al.*'s measurement in guinea pig was made at a position with a cf of 18 kHz, and our stiffness measurements in gerbil were made at approximately the 17-kHz cf position.

IV. SUMMARY

Our measurements of basilar membrane stiffness as a function of basilar membrane displacement, made in the base of the gerbil cochlea, revealed two regions in which the stiffness was approximately constant over several microns, followed by a region of quadratically increasing stiffness. The extent and magnitude of the initial stiffness plateau suggest that this plateau is due to soft structures of the basilar membrane that have a low resistance to shear but, as Miller stated, might be incompressible under pressure loading. Then, the second stiffness plateau, with a value of approximately 9 N/m, is the relevant stiffness for cochlear mechan-

ics. We did not find differences in the stiffness pre-mortem versus early post-mortem. However, the one animal that was outstanding in maintaining a viable CAP through two stiffness versus displacement measurements also possessed the largest second plateau stiffnesses, the largest being 20 N/m. This suggests that healthier cochleas possess a greater stiffness.

ACKNOWLEDGMENTS

The authors are grateful to Ruth Anne Eatock and Hideo Nakajima for their thorough readings and criticisms of the early manuscript. The work present here was supported by a National Research Service Award from the National Institute of Neurological and Communication Disorders and the National Institute on Deafness and Other Communication Disorders.

APPENDIX A: DETERMINATION OF VOLUME COMPLIANCE

The linear beam equation, appropriate for distortions less than 0.3 times the beam height, is

$$\frac{Dd^4y}{dx^4} = q, \quad (\text{A1})$$

where D is the flexural rigidity of the beam, a function of the beam height, width, and material, and D has units ($N \cdot m$); y is the distortion perpendicular to undistorted beam length (m); x is the distance along the undistorted beam (m); q is the external surface force (N/m^2); s is the beam length = basilar membrane width = $175 \mu\text{m}$; and d is the probe diameter = beam width = $25 \mu\text{m}$.

A derivation of the beam equation can be found in Symon (1971). The boundary conditions are either such that the edges are clamped ($dy/dx = 0$ at $x = 0$ and $x = s$) or such that the edges are simply supported ($d^2y/dx^2 = 0$ at $x = 0$ and $x = s$). In both cases $y = 0$ at $x = 0$ and $x = s$.

When the force is due to a pressure P , applied evenly over the beam, the solution to the beam equation is:

clamped boundary condition:

$$y = \frac{P}{D} \left\{ \frac{x^4}{24} - x^3 \left(\frac{s}{12} \right) + x^2 \left(\frac{s^2}{24} \right) \right\}. \quad (\text{A2a})$$

simply supported boundary condition:

$$y = \frac{P}{D} \left\{ \frac{x^4}{24} - x^3 \left(\frac{s}{12} \right) + x \left(\frac{s^3}{24} \right) \right\}. \quad (\text{A2b})$$

Volume compliance = (displaced volume per unit length)/pressure = displaced area/pressure. To find the displaced area we take the integral $\int_0^s y dx$. We find for the volume compliance:

clamped boundary condition:

$$A/P = s^5/D[0.0014]. \quad (\text{A3a})$$

simply supported boundary condition:

$$A/P = s^5/D[0.0083]. \quad (\text{A3b})$$

When the force is equal to a surface force q applied over an area of size d^2 at the center of the beam, the deflection of the center of the beam was found in Gummer *et al.* Using the result, the point compliance, equal to the center displace-

ment y , divided by applied force F , is clamped boundary condition:

$$y/F = [s^4/(d^2D)][0.00069]. \quad (\text{A4a})$$

simply supported boundary condition:

$$y/F = [s^4/(d^2D)][0.0029]. \quad (\text{A4b})$$

The results from Eqs. (A3) and (A4) can be combined to express volume compliance in terms of point compliance. The result is

clamped boundary condition:

$$\begin{aligned} \text{volume compliance} &= \text{point compliance} \times sd^2 \\ &\times [0.0014/0.00069] \\ &= \text{point compliance} \times 2.2 \times 10^{-13} \text{ m}^3. \end{aligned} \quad (\text{A5a})$$

simply supported boundary condition:

$$\begin{aligned} \text{volume compliance} &= \text{point compliance} \times sd^2 \\ &\times [0.0083/0.0029] \\ &= \text{point compliance} \times 3.1 \times 10^{-13} \text{ m}^3. \end{aligned} \quad (\text{A5b})$$

APPENDIX B: PROBE DESIGN AND CALIBRATION

1. Design

The probe is illustrated in Fig. B1. The two major components of the probe are a force-to-voltage transducer and a voltage-to-displacement transducer. Both transducers employ piezoelectric bimorphs (Vernitron, Bedford, Ohio). The voltage-to-displacement transducer (driver) is used to vary both the static and dynamic positions of the force-to-voltage transducer in the range from 0.001–100 μm at frequencies up to 100 Hz. The force transducer is capable of detecting ac return forces, before signal averaging, on the order of 10 nN. Both the driver and force transducer behave linearly over the ranges of motion relevant in the experiments.

Two $3.0 \times 0.65 \times 0.05$ -cm bimorphs served as the driver. They were secured between the rod which is used to attach

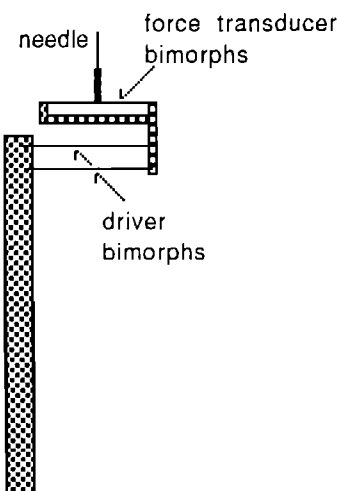


FIG. B1. Force probe. Side view shows bimorphs edge on; nulling bimorph is mounted next to force bimorph with attached needle. Speckled regions are aluminum mounting structure. The probe needle is 1.8 cm long and has a tip diameter of 25 μm .

the probe to the setup and the structure that holds the force transducer bimorphs. Voltage was applied to the driver bimorphs in a manner that allows for secure attachments between the driver bimorphs and the attached structures, an arrangement that has been described by Howard and Hudspeth (1988) and Murali *et al.* (1986). Information on the use of bimorphs as motion sources was published by Corey and Hudspeth (1980).

The force transducer comprised two identical $2.5 \times 0.32 \times 0.05$ -cm bimorphs: a force and a nulling bimorph, mounted side-by-side in an aluminum structure. A thin stainless steel needle was glued onto the center of one bimorph, the force bimorph. The needle was sharpened and the tip was flattened to a diameter of 25 μm . The nulling bimorph was required to cancel the voltage generated across the force bimorph by the distortion caused by the bimorph's own inertia. With sinusoidal excursion the force on both the force and nulling bimorphs due to their inertias will be

$$F = mw^2 dx, \quad (\text{B1})$$

where m is the mass of the bimorph, w is 2π multiplied by the excursion frequency and dx is the excursion size. The mass of a single transducer bimorph is approximately 250 mg. With a frequency of 70 Hz, from Eq. (B1), the inertial force is equal to 48 N/m dx . This inertial force is roughly 50 times the size of the force we measure due to basilar membrane stiffness. Therefore, before contacting the basilar membrane, the force transducer structure was put through a 1- μm peak excursion with frequency equal to the frequency at which the stiffness measurement will be made. The inertial voltages of the two bimorphs that comprise the force transducer were nulled in a summing amplifier following a first stage charge amplifier. Nulling was good to 1 part in 500 and was stable for hours (periods longer than experimental runs).

The force and nulling bimorphs were electrically shielded. A thin layer of silicone sealer insulated the surface of the bimorph. The insulated surfaces were coated with silver paint, and grounded.

2. Calibration

1. Motion calibration

The static motion of the driver was calibrated by viewing the needle tip through the calibrated eyepiece micrometer of a microscope while applying dc voltage to the driver bimorphs. The static displacement was approximately 0.45 μm per volt. The motion to voltage ratio was approximately constant over at least 30 μm of static position, although creep or hysteresis could produce up to 10% error in repeatability and stability in the static position. The dynamic excursion of the driver, measured as for static motion excursions greater than 1 μm , was approximately 0.42 μm per volt at 70 Hz. At frequencies above 100 Hz, the excursion grew as the frequency approached a 180-Hz resonance. Both the static and the dynamic motion appeared in line with the needle axis at frequencies up to and through the 180-Hz resonance. Higher frequency resonances had substantial transverse components. Scaling of the excursion level with voltage level, and the excursion versus frequency relation-

ship were determined (following a method outlined in Corey and Hudspeth, 1980) by projecting a magnified image of the needle onto a photodiode (EE&G PV-215) and referencing the voltage output of the photodiode at various drive levels and frequencies to the output for a known excursion. The excursion level scaled linearly with driver voltage in the range of voltages and frequencies measured: peak driver voltages from 50 mV to 5 V and frequencies from 35–100 Hz. With a constant magnitude driving voltage, the excursion size increased by 20% between 5 and 100 Hz.

Measurements were made to insure that the static position (dc voltage applied to driver) did not influence the dynamic excursion size, or diminish the precision of inertial nulling.

2. Sensitivity (V/N) calibration

The force transducer's sensitivity was determined by measuring its voltage output in measurements on three samples of known stiffness. The stiffnesses of the samples were 63.0, 42.9, and 10.7 N/m. The force transducer needle was brought into contact with each of the samples and, using the driver, it was put through 5- and 25-nm peak 80-Hz excursions. The restoring force exerted by the materials on the needle was found by multiplying their stiffnesses by the excursion size. The magnitude and phase of the force transducer's output due to the restoring force of the samples was measured. The magnitude scaled linearly with excursion amplitude. With two of the samples the phase of the transducer voltage was within 2° of 180° relative to the driver motion. The phase of the restoring force of a pure stiffness is 180°. With the third sample, the phase was within 14° of 180°. It is probable that the phase discrepancy was due to a mechanical resonance of the sample. The voltage output of the force transducer was divided by the restoring force to give the bimorph sensitivity in volts per newton. The different calibration materials gave sensitivities of 14.66, 16.19, and 14.24 V/N with a mean of 15.03 V/N. The probe calibration was stable over time, given that this calibration provided a value similar to the 15.8-V/N value obtained 9 months earlier.

A check on the calibrated sensitivity was provided by the output of a single (unnulling) force transducer bimorph due to its own inertial force, which gave the transducer sensitivity as 17.3 V/N, quite close to our 15.03- and 15.8-V/N calibrations.

The theoretical sensitivity of bimorph transducers, based on their distortions under specific mounting conditions and loads, was given in Thurston (1953). The predicted sensitivity of a bimorph with the dimensions and piezoelectric material of our transducer bimorph, beam mounted with simply supported boundary conditions, was 30 V/N. Our bimorph is beam mounted, but with clamped boundary conditions, which, by reducing the distortion to a given force, will reduce the sensitivity relative to the sensitivity of a simply supported bimorph. Therefore, our calibrated sensitivity is reasonably consistent with the theoretical sensitivity.

3. Probe stiffness

The probe stiffness is equal to the series combination of the driver and transducer stiffnesses. The stiffness of the driver was estimated by measuring the change in inertial voltage of the nulling force transducer bimorph when the needle was in contact with an object with stiffness small, but not insignificant, relative to the stiffness of the probe. The change in the inertial voltage of the nulling transducer when the probe was loaded by an object, relative to the voltage when the probe was unloaded was due to a reduction in probe motion. The ratio of loaded motion to unloaded motion is

$$x_1/x_0 = k_d / (k_d + k_{ot}), \quad (B2)$$

where k_d is the driver stiffness and k_{ot} is the series combination of the transducer stiffness (k_t) and the object stiffness (k_o). An object with a stiffness of 256 N/m was found to reduce the motion of the probe to 0.944 times its unloaded motion. Because the transducer stiffness was expected to be much larger than 256 N/m, k_{ot} was approximately equal to $k_o = 256$ N/m. The stiffness of the driver found from Eq. (B2) was $k_d = 4315$ N/m.

Because of the relatively small size and stiff mounting of the force transducer bimorphs, the stiffness of the force transducer is expected to be substantially larger than the stiffness of the driver. Applying an expression for bimorph stiffness from Corey and Hudspeth (1980) to the specific mounting conditions of the transducer bimorphs gave a predicted force transducer stiffness of 18 700 N/m. The probe stiffness, found as the series combination of the driver and transducer stiffnesses, is approximately 3500 N/m.

- Allaire, P., Raynor, S., and Billone, M. (1974). "Cochlear partition stiffness—A composite beam model," *J. Acoust. Soc. Am.* **55**, 1252–1258.
- Bekesy, G., von (1960). *Experiments in Hearing*, edited and translated by E. G. Wever (McGraw Hill, New York), Chap. 11, pp. 469–476.
- Corey, D. P., and Hudspeth, A. J. (1980). "Mechanical stimulation and micromanipulation with piezoelectric bimorph elements," *J. Neurosci. Methods* **3**, 183–202.
- Dancer, A., and Frank, R. (1980). "Intracochlear sound pressure measurements in guinea pigs," *Hear. Res.* **2**, 191–205.
- Gummer, A. W., Johnstone, B. M., and Armstrong, N. J. (1981). "Direct measurements of basilar membrane stiffness in the guinea pig," *J. Acoust. Soc. Am.* **70**, 1298–1309.
- Howard, J., and Hudspeth, A. J. (1988). "Compliance of the hair bundle associated with gating of the mechanoelectric transduction channels in the bullfrog's saccular hair cell," *Neuron* **1**, 189–199.
- Iurato, S. (1962). "Functional implications of the nature and submicroscopic structure of the tectorial and basilar membranes," *J. Acoust. Soc. Am.* **34**, 1386–1395.
- Khanna, S. M., and Leonard, D. G. B. (1986). "Relationship between basilar membrane and hair cell condition," *Hear. Res.* **23**, 55–70.
- Lay, D. M. (1972). "The anatomy, physiology, functional significance and evolution of specialized hearing organs of gerbilline rodents," *J. Morph.* **138**, 41–120.
- Miller, C. E. (1985). "Structural implications of basilar membrane compliance measurements," *J. Acoust. Soc. Am.* **77**, 1465–1474.
- Muralt, P., Pohl, D. W., and Denk, W. (1986). "Wide-range, low-operating-voltage, bimorphs STM: application as potentiometer," *IBM J. Res. Dev.* **30**, 443–450.
- Nedzelinsky, V. (1980). "Sound pressures in the basal turn of the cat cochlea," *J. Acoust. Soc. Am.* **68**, 1676–1689.
- Plassman, W., Peetz, W., and Schmidt, M. (1987). "The cochlea in gerbilline rodents," *Brain Behav. Evol.* **30**, 82–102.
- Rhode, W. S., and Robles, L. (1974). "Evidence from Mossbauer experiments for nonlinear vibration in the cochlea," *J. Acoust. Soc. Am.* **55**, 588–596.

- Ruggero, M. A., Rich, N. C., Robles, L., and Shivapuja, B. G. (1990). "Middle ear responses in the chinchilla and its relationship to mechanics at the base of the cochlea," *J. Acoust. Soc. Am.* **87**, 1612-1619.
- Sellick, P. M., Patuzzi, R., and Johnstone, B. M. (1982). "Measurement of basilar membrane motion in the guinea pig using the Mossbauer technique," *J. Acoust. Soc. Am.* **72**, 131-141.
- Strelioff, D., and Flock, A. (1984). "Stiffness of sensory-cell hair bundles in the isolated guinea pig cochlea," *Hear. Res.* **15**, 119-28.
- Symon, K. R. (1971). *Mechanics* (Addison-Wesley, Reading, MA), pp. 241-247.
- Thurston, E. G. (1953). "The theoretical sensitivity of three types of rectangular bimorph transducers," *J. Acoust. Soc. Am.* **25**, 870-872.
- Voldrich, L. (1978). "Mechanical properties of the basilar membrane," *Acta Oto-Laryngol.* **86**, 331-335.